

## Journal Pre-proofs

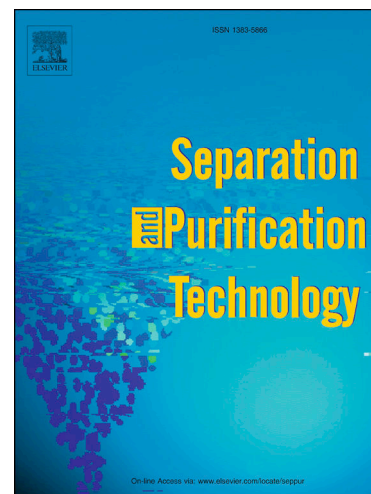
Enhanced absorption separation of hydrofluorocarbon/hydrofluoroolefin refrigerant blends using ionic liquids

Salvador Asensio-Delgado, Fernando Pardo, Gabriel Zarca, Ane Urriaga

PII: S1383-5866(20)31610-5  
DOI: <https://doi.org/10.1016/j.seppur.2020.117136>  
Reference: SEPPUR 117136

To appear in: *Separation and Purification Technology*

Received Date: 3 January 2020  
Revised Date: 24 March 2020  
Accepted Date: 19 May 2020



Please cite this article as: S. Asensio-Delgado, F. Pardo, G. Zarca, A. Urriaga, Enhanced absorption separation of hydrofluorocarbon/hydrofluoroolefin refrigerant blends using ionic liquids, *Separation and Purification Technology* (2020), doi: <https://doi.org/10.1016/j.seppur.2020.117136>

This is a PDF file of an article that has undergone enhancements after acceptance, such as the addition of a cover page and metadata, and formatting for readability, but it is not yet the definitive version of record. This version will undergo additional copyediting, typesetting and review before it is published in its final form, but we are providing this version to give early visibility of the article. Please note that, during the production process, errors may be discovered which could affect the content, and all legal disclaimers that apply to the journal pertain.

© 2020 Published by Elsevier B.V.

© 2020 This manuscript version is made available under the CC-BY-NC-ND 4.0 license <http://creativecommons.org/licenses/by-nc-nd/4.0/>

Enhanced absorption separation of  
hydrofluorocarbon/hydrofluoroolefin refrigerant blends using ionic  
liquids

**Authors:**

**Salvador Asensio-Delgado, Fernando Pardo, Gabriel Zarca\*, Ane Urtiaga**

Department of Chemical and Biomolecular Engineering, Universidad de Cantabria,  
Av. Los Castros 46, Santander 39005, Spain.

\*Corresponding author e-mail address: [zarcag@unican.es](mailto:zarcag@unican.es)

Full text

Submitted to Separation and Purification Technology

January 2020

**Abstract**

The separation of hydrofluorocarbons (HFCs) and hydrofluoroolefins (HFOs) from novel refrigerant blends will become essential to boost the recycling of these compounds and drastically reduce the emission of HFCs, which are powerful greenhouse gases. In this work, the use of ionic liquids (ILs) as solvent media is explored to perform the selective separation of HFC/HFO refrigerant mixtures composed of the HFCs R32 (difluoromethane) and R134a (1,1,1,2-tetrafluoroethane) and the HFO R1234yf (2,3,3,3-tetrafluoropropene). The low-viscosity IL 1-ethyl-3-methylimidazolium thiocyanate, [C<sub>2</sub>mim][SCN], is selected as separation agent to prove that small and non-fluorinated ILs, with lower hydrogen bonding capability than other ILs, can provide enhanced solubility selectivity and mass transport properties for the selective separation of HFC/HFO refrigerant blends. The phase behavior of IL-refrigerant systems is determined at temperatures between 283.15 and 313.15 K and pressures up to 0.7 MPa. Results are parametrized according to the NRTL activity model and the separation selectivity is assessed in terms of Henry's law constants, solvation enthalpies and entropies, infinite dilution coefficients, Gibbs free energy of mixing, and ideal and noncompetitive selectivity. Results show superior HFC/HFO solubility selectivity in [C<sub>2</sub>mim][SCN] compared to other ILs due to unfavorable entropic effects that difficult the solvation of large molecules such as R1234yf.

**Keywords**

Difluoromethane, ionic liquid, NRTL model, solubility selectivity, 1,1,1,2-tetrafluoroethane, 2,3,3,3-tetrafluoropropene

## 1. Introduction

Hydrofluorocarbons (HFCs) are a family of compounds with excellent refrigerant properties that substituted ozone-depleting substances, namely, chlorofluorocarbons (CFCs) and hydrochlorofluorocarbons (HCFCs), whose production and use were phased out under the Montreal Protocol. Therefore, the concentration of HFCs in the atmosphere has raised more than twofold since 1990 as a consequence of their massive introduction to the market as refrigerants, fire retardants, foam blowing agents and propellants [1]. Once established on the market, emissions of HFCs are steadily increasing due to fugitive emissions, the lack or non-application of end-of-life recovery protocols, and the low share of refrigerant recycling [2]. However, despite having negligible ozone depletion potentials (ODPs), HFCs are still concerning greenhouse gases with extremely high global warming potentials (GWPs), up to several orders of magnitude higher than that of the reference CO<sub>2</sub> (GWP = 1) [3,4]. For this reason, new legislation and international agreements have recently entered into force. Mainly, Regulation EU 517/2014 in Europe has scheduled the progressive HFCs phase-down, and the Kigali Amendment to Montreal Protocol, already adopted by 93 parties, aims at reducing HFCs emissions by 80% with respect to 1990 levels by 2045 [5–7].

Accordingly, there are several HFC blends commercialized as refrigerants that will be phased-out due to their high GWP (e.g., R404A, R407C, R410A, and R507C). To meet current legislation requirements, new refrigerant mixtures containing hydrofluoroolefins (HFOs), unsaturated hydrofluorocarbons that exhibit very low GWP, are being formulated and incorporated into the refrigerant market as environmentally friendly alternatives (e.g., R448A, R449A, R454A, R455A, and R513A). The composition of the aforementioned mixtures and their GWP is provided in Table S1 as Supplementary Information. In addition, Table 1 presents relevant properties of the main HFCs and HFOs that are being used in new HFC/HFO blends [2,3,8].

The current legal framework provides an excellent opportunity to focus technological innovations on the design of refrigerant recovery processes to shift the refrigeration and air conditioning (RAC)

industry towards a more circular economy [9]. To promote the recycling of refrigerants, blend components must be recovered as pure compounds so they can be then reused in the formulation of new more environmentally friendly commercial blends. However, some relevant HFC+HFO systems behave almost like pure fluids with virtually no variation of composition between the vapor and liquid phases and almost constant evaporation/condensation temperature at a given pressure (i.e., the temperature glide is lower than 1 K). This is for instance the case of systems R134a+R1234yf, R134a+R1234ze(E) and R134+R1234ze(E). Other important systems also exhibit near-azeotropic behavior at some point, e.g., system R32+R1234yf, and therefore, it may be difficult to recover their individual components at the high purity needed for reuse [10–13]. These reasons make the separation of those refrigerant systems by means of conventional distillation very challenging or even impossible [14].

Table 1. Properties of common HFCs and HFOs contained in new refrigerant blends [8].

Properties	HFCs			HFOs	
	R32	R125	R134a	R1234yf	R1234ze(E)
Molecular formula	CH <sub>2</sub> F <sub>2</sub>	C <sub>2</sub> HF <sub>5</sub>	C <sub>2</sub> H <sub>2</sub> F <sub>4</sub>	C <sub>3</sub> H <sub>2</sub> F <sub>4</sub>	C <sub>3</sub> H <sub>2</sub> F <sub>4</sub>
GWP	675	3500	1430	4	6
Molar mass (g mol <sup>-1</sup> )	52.02	120.02	102.03	114.04	114.04
Critical temperature (K)	351.26	339.17	374.21	367.85	382.52
Critical pressure (bar)	57.82	36.18	40.59	33.82	36.35
Critical volume (cm <sup>3</sup> mol <sup>-1</sup> )	122.70	209.25	199.32	239.81	233.10
Acentric factor	0.2769	0.3052	0.3268	0.2760	0.3131
Normal boiling point (°C)	-51.65	-48.09	-26.07	-29.45	-18.95
ASHRAE-34 flammability	A2L	A1	A1	A2L	A2L

In contrast, the development of extractive distillation processes for the separation of HFCs/HFOs based on gas solubility differences appears as a more effective alternative [15]. Moreover, ionic liquids (ILs) have been proposed as a novel solvent platform in new gas separation processes owing to their unique features, e.g., extremely low vapor pressure, high thermal and chemical stability, liquid state in a wide

temperature range, and enhanced solvation properties, among others [16–18]. Several studies have been conducted to assess the phase equilibria of binary systems of fluorinated refrigerants and ILs [14,19–33]. However, the design of novel gas separation processes for the recovery of refrigerants requires a deep understanding of both the refrigerant-IL phase behavior and mass transport phenomena, which can severely affect the process efficiency [34]. In this sense, a preliminary assessment of published data is performed in Table 2, which shows the Henry's law constants at infinite dilution of the gases studied in this work in several ILs, along with the IL molar volume and viscosity. As can be seen, for a given solute, solubility increases with IL molar volume and fluorination of the anion. Moreover, these trends are particularly significant for the HFO R1234yf, whose solubility is consistently lower than that of R32 and R134a. In addition, to date, solubility data for all these refrigerant gases in low viscosity ILs have not been reported. Consequently, it is expected that an IL that combines a small non-fluorinated anion and a cation with a short alkyl chain would significantly decrease the HFO solubility and provide enhanced HFC/HFO selectivity and improved mass transfer rates. Therefore, the IL 1-ethyl-3-methylimidazolium thiocyanate,  $[C_2mim][SCN]$ , is selected in the present work because of its low molar volume ( $151.52 \text{ cm}^3 \text{ mol}^{-1}$ ), the absence of fluorine atoms and its very low viscosity compared to other ILs ( $24.5 \text{ mPa s}$  at  $298 \text{ K}$ ) [35,36]. The thermodynamic absorption equilibria of R32, R134a and R1234yf in  $[C_2mim][SCN]$  are assessed and modeled using the NRTL activity method to allow simulation of an extractive distillation separation process in a further stage. Moreover, the diffusion coefficients of each refrigerant gas are evaluated at several temperatures and compared to those found in other systems. Finally, a thermodynamic assessment is performed to gain a deeper understanding on the refrigerant solvation in ILs and the importance of adequate IL selection for designing novel separation processes.

Table 2. Henry's law constants of R32, R134a and R1234yf in several ILs at 300 K [18,19,26–28,32,37–49].

		Ionic liquid		Henry's law constants (MPa)		
Anion	Cation	Molar volume (cm <sup>3</sup> mol <sup>-1</sup> )	Viscosity (mPa s)	HFC-R32	HFC-R134a	HFO-R1234yf
[BF <sub>4</sub> ]	[C <sub>2</sub> mim]	154.27	38.8			15.56
	[C <sub>4</sub> mim]	188.10	103.5	1.32		
	[C <sub>6</sub> mim]	222.08	206		0.90	4.57
[PF <sub>6</sub> ]	[C <sub>4</sub> mim]	207.82	282	1.21	1.22	5.24
	[C <sub>6</sub> mim]	241.26	483		0.96	4.30
[Tf <sub>2</sub> N]	[C <sub>2</sub> mim]	257.70	33.9	0.96	0.73	
	[C <sub>6</sub> mim]	326.20	70.1	0.72	0.63	1.65

## 2. Experimental

### 2.1. Materials

The IL [C<sub>2</sub>mim][SCN] (98%) was purchased from IoLiTec and dried under vacuum during 48 h before used. The water content of [C<sub>2</sub>mim][SCN] was determined using Karl Fischer titration to be <200 ppm. R32 (99.9%) was purchased from Coproven Climatización (Gas Servei licensed supplier, Spain). R134a (99.8%) and R1234yf (99.9%) were supplied by Carbueros Metálicos (Air Products).

### 2.2. Procedure

Gas absorption into ILs was measured using an isochoric saturation method, which relies on gas-phase measurements. The experimental system was described in detail in our previous works [16,17,35]. It consists of a jacketed stirred tank reactor (Buchi, model Picoclave type 1/100 mL) equipped with a pressure transducer (Aplisens, model PCE-28, 0.2% accuracy) and a Pt-100 temperature sensor connected to a cryothermostatic bath (Julabo, model F25-ME, ±0.01 K). A storage cylinder of known volume equipped with an absolute digital manometer (Keller, model Leo 2, 0.1% accuracy at full scale) is used as gas reservoir. The reactor was loaded with ~10 g (±0.0001 g) of IL and degassed at 333 K applying vacuum for 4-6 h before each absorption experiment. Initially, absorption was allowed to proceed without stirring for the first 20 minutes for diffusivity measurements. After that, the stirrer was set to 500 rpm and gas absorption proceeded until the system reached equilibrium conditions. It was assumed that equilibrium was reached when pressure remained constant for more than 20

minutes. The amount of gas absorbed in each step ( $n_i$ ) and the accumulated absorbed amount ( $n_{abs}$ ) were calculated as follows:

$$n_i = \rho_{(i,s)} \cdot V_s + \rho_{(i-1,r)} \cdot (V_r - V_l) - \rho_{(i,eq)} \cdot (V_s + V_r - V_l) \quad (1)$$

$$n_{abs} = n_i + \sum_{k=1}^{i-1} n_k \quad (2)$$

where  $V_s$ ,  $V_r$  and  $V_l$  are the storage, reactor and loaded IL volumes, respectively, and  $\rho_{i,s}$ ,  $\rho_{i-1,r}$  and  $\rho_{i,eq}$  are the gas molar densities in the storage cylinder, in the reactor and at equilibrium conditions, respectively. Molar densities were calculated from pressure and temperature data using the Peng-Robinson equation of state to account for deviations from ideal behavior. The molar fraction of gas dissolved in the IL is defined as:

$$x = \frac{n_{abs}}{n_l + n_{abs}} \quad (3)$$

where  $n_l$  are the moles of IL. To validate the accuracy of our system, we performed absorption experiments of R1234yf in  $[C_2mim][BF_4]$  achieving excellent agreement with data available in literature [19] as shown in Figure S1 of the Supplementary Information.

### 2.3. Modeling

Modeling the absorption equilibria is essential for the simulation of absorption systems with computer tools used for process design. We present here the model parameters of the absorption equilibria of the three hydrofluorocarbon gases in  $[C_2mim][SCN]$  using the non-random two-liquid (NRTL) model [18,50,51]. According to this activity coefficient based model, vapor-liquid equilibria is calculated as

$$y_i p \Phi = x_i \gamma_i p_i^s \quad (i \in \mathbb{Z} [1, N]) \quad (4)$$

where  $y_i$  and  $x_i$  are molar fractions of the  $i$  species in vapor and liquid phases, respectively, and  $\gamma_i$  and  $p_i^s$  are the activity coefficient and vapor pressure, respectively. The correction factor  $\Phi$  is calculated as follows:

$$\Phi = \exp \left[ \frac{(B_i - V_i^l)(p - p_i^s)}{RT} \right] \quad (5)$$

where  $R$  is the ideal gas constant,  $B_i$  is the second virial coefficient and  $V_i^l$  is the saturated liquid molar volume.  $p_i^s$ ,  $B_i$  and  $V_i^l$  were calculated using CoolProp 6.3.0 software [8]. Combination of Eqs. (4) and (5) leads to the following expression of the activity coefficients:

$$\gamma_1 = \frac{p}{x_1 p_1^s} \exp \left[ \frac{(B_1 - V_1^l)(p - p_1^s)}{RT} \right] \quad (6)$$

NRTL minimizes the difference between this experimental activity coefficient and the calculated as

$$\ln \gamma_1 = x_2^2 \left[ \tau_{21} \left( \frac{G_{21}}{x_1 + x_2 G_{21}} \right)^2 + \frac{\tau_{12} G_{12}}{(x_2 + x_1 G_{12})^2} \right] \quad (7)$$

where  $G_{12} = \exp(-\alpha\tau_{12})$ ,  $G_{21} = \exp(-\alpha\tau_{21})$ ,  $\tau_{12} = \tau_{12}^0 + \tau_{12}^1/T$  and  $\tau_{21} = \tau_{21}^0 + \tau_{21}^1/T$ . Thus, the model parameters to be optimized are  $\alpha$ ,  $\tau_{12}^0$ ,  $\tau_{12}^1$ ,  $\tau_{21}^0$  and  $\tau_{21}^1$ .

#### 2.4. Diffusivity

Diffusion coefficients were calculated using the semi-infinite volume model [52,53].

$$\frac{\partial C}{\partial t} = D \frac{\partial^2 C}{\partial y^2} \quad (8)$$

where  $C$  expresses the concentration of gas in solution,  $t$  is time,  $D$  is the diffusion coefficient and  $y$  is the depth into the IL. Integration of Eq. (8) leads to the accumulated dissolved moles per unit area from which diffusion coefficients are obtained:

$$M_t = \int_0^t \left( D \left( \frac{\partial C}{\partial y} \right)_{y=0} \right) dt = \sqrt{D} \left( 2C_{y=t=0} \sqrt{\frac{t}{\pi}} - \frac{1}{2} m t \sqrt{\pi} \right) = \sqrt{D} \varepsilon \quad (9)$$

where  $C_{y=t=0}$  is the initial concentration in the surface and  $m$  is a mass transfer coefficient, both of them calculated according to

$$C_{y=0} = C_{y=t=0} + m\sqrt{t} \quad (10)$$

where  $C_{y=0}$  is the surface concentration defined as [54]

$$C_{y=0} = \frac{\rho_{IL}}{M_{IL} \cdot \left( \frac{k_H}{f} - 1 \right)} \quad (11)$$

where  $\rho_{IL}$  and  $M_{IL}$  are density and molar mass of the IL, respectively.

### 2.5. Separation assessment

The Henry's law constants ( $k_H$ ) are calculated from the experimental data as follows:

$$k_H(T) = \lim_{x \rightarrow 0} \frac{f(P, T)}{x} \quad (12)$$

where  $f$  is the refrigerant fugacity calculated using PR-EoS. As Henry's law constants are defined at infinite dilution, Eq. (12) can be simplified to [18,25]

$$k_H \approx \left( \frac{df}{dx} \right)_{x=0} \quad (13)$$

Solvation enthalpy,  $\Delta H_{sol}$ , and entropy,  $\Delta S_{sol}$ , provide information regarding the strength of interaction between the IL and gas and the ordering in the mixture [55,56]. Henry's law constants allow calculation of solvation enthalpies and entropies at infinite dilution using the van't Hoff equation [57]:

$$\Delta H_{sol} = R \left( \frac{\partial \ln k_H}{\partial \left( \frac{1}{T} \right)} \right)_p \quad (14)$$

$$\Delta S_{sol} = -R \left( \frac{\partial \ln k_H}{\partial \ln T} \right)_p \quad (15)$$

The comparison of solvation energies gives information regarding solubility differences between gases that is very useful for an initial assessment of the expected selectivity provided by a certain IL. Besides,

Henry's law constants can be used to calculate the ideal selectivity at infinite dilution,  $S_{1/2}$ , defined as [55]

$$S_{1/2} = \frac{1/k_{H,1}}{1/k_{H,2}} = \frac{k_{H,2}}{k_{H,1}} \quad (16)$$

At higher pressures, a non-competitive selectivity can be defined from VLE data as

$$S_{1/2}^P = \frac{y_2/x_2}{y_1/x_1} = \frac{x_1}{x_2} \quad (17)$$

where the vapor phase,  $y_i = 1$ , owing to the negligible vapor pressure of ILs.

Further understanding of the separation mechanism involves the analysis of thermodynamic properties related to solute and solvent interactions. NRTL model allows for the calculation of these interaction parameters. Fugacity coefficients at infinite dilution ( $\gamma_1^\infty$ ) are calculated from Eq. (7) when  $x_1 = 0$  and  $x_2 = 1$ .

$$\ln \gamma_1^\infty = \tau_{21} + \tau_{12}G_{12} \quad (18)$$

Finally, Gibbs free energy of mixing is derived as the sum of the ideal contribution and the excess energy:

$$\Delta g^{mix} = \Delta g^{id} + \Delta g^{ex} \quad (19)$$

where both contributions are calculated as follows:

$$\Delta g^{id} = RT(x_1 \ln x_1 + x_2 \ln x_2) \quad (20)$$

$$\Delta g^{ex} = RT(x_1 \ln \gamma_1 + x_2 \ln \gamma_2) \quad (21)$$

### 3. Results and discussion

#### 3.1. Gas solubility

In this section, the absorption of R32, R134a and R1234yf in [C<sub>2</sub>mim][SCN] is presented. The solubility data were measured at temperatures between 283.15 and 313.15 K and pressures up to 0.7 MPa. The results are plotted in Figure 1. Also, Tables S2-S4 of the Supplementary information present the solubility data of each system expressed as molar fraction and molality, which is a more adequate unit for process design [58], along with the related uncertainties calculated by the propagation-of-errors method. As can be seen, the molar fraction of gas absorbed in the IL increases, as expected, when temperature decreases and pressure increases. The comparison between refrigerants reveals that the HFCs R32 and R134a exhibit much higher solubility in [C<sub>2</sub>mim][SCN] than the HFO R1234yf. This solubility difference is of great relevance to design selective absorption processes in which R32, or R134a, is preferentially absorbed into the IL while the HFO primarily remains in the gas phase.

Figure 1 shows that the phase equilibria of HFC/HFO + IL systems are correlated with very good accuracy using the conventional NRTL activity model for nonelectrolyte solutions, which is in good agreement with previous works that also treated ILs as undissociated species [18]. Table 3 presents the model parameters, the calculated absolute average relative deviation in activity coefficients ( $AAR_{D_\gamma}$ ) and the root-mean-square deviation in pressure (RMSD) for each system. The parameter  $\alpha$  characterizes the tendency of two species to distribute in an organized way, where the system is ordered if  $\alpha = 0$  and immiscibility is predicted if  $\alpha > 0.426$ . Although  $\alpha$  can be treated as an adjustable parameter, for the case of fluorocarbons and hydrocarbons  $\alpha$  is usually assumed constant and equal to 0.2 [18,50,59], and therefore, we decided to follow this approach for consistency with previous works. The parameters  $\tau_{12}^1$  and  $\tau_{21}^1$  represent the excess free energy of Gibbs divided by the ideal gas constant, while  $\tau_{12}^0$  and  $\tau_{21}^0$  lack physical meaning and are used to correct deviations from the ideal behavior [18]. In this way, the absorption of R32 and R134a was modeled using only two adjustable

parameters ( $\tau_{12}^1$  and  $\tau_{21}^1$ ), while the absorption of R1234yf required all four adjustable parameters to be accurately modeled.

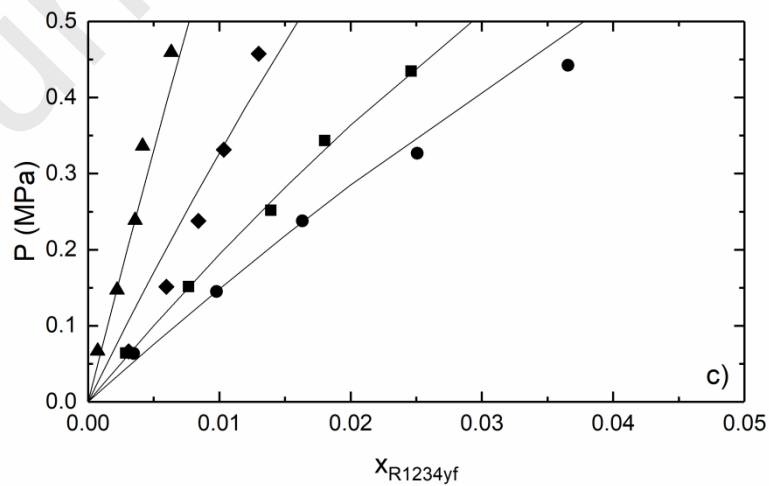
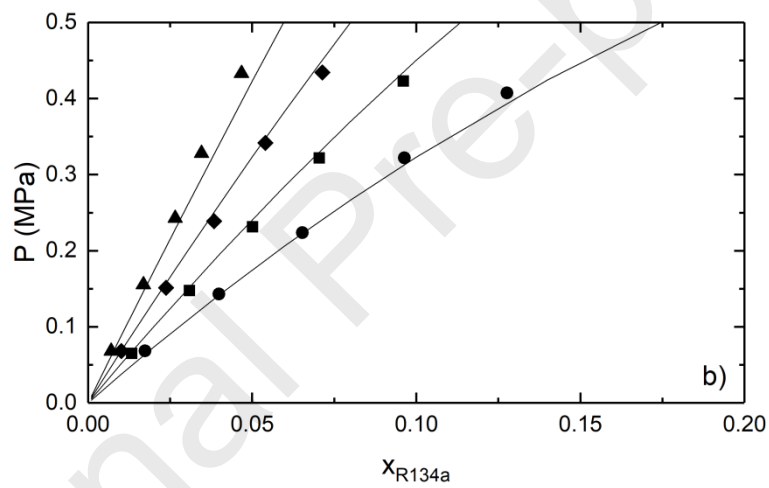
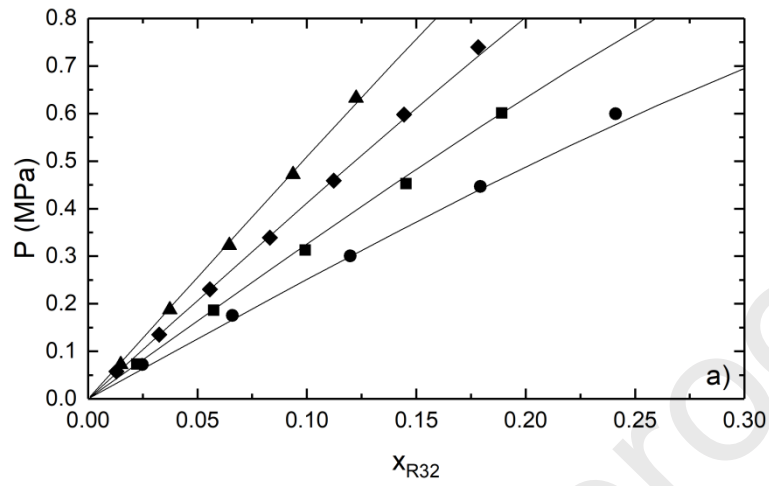


Figure 1. Solubility of common refrigerant gases in [C<sub>2</sub>mim][SCN] at several temperatures: 283.15 (●), 293.15 (■), 303.15 (◆) and 313.15 K (▲). a) R32, b) R134a and c) R1234yf. Solid lines represent NRTL model calculations.

Table 3. NRTL activity model parameters for the absorption of fluorinated gases in [C<sub>2</sub>mim][SCN].

	R32 + [C <sub>2</sub> mim][SCN]	R134a + [C <sub>2</sub> mim][SCN]	R1234yf + [C <sub>2</sub> mim][SCN]
$\alpha$	0.2	0.2	0.2
$\tau_{12}^0$	0	0	179.52
$\tau_{12}^1$	1025.6	2682.6	-47781
$\tau_{21}^0$	0	0	21.89
$\tau_{21}^1$	-210.04	254.58	-5506.8
<b>RMSE (MPa)</b>	0.009	0.013	0.029
<b>AARD<sub>y</sub> (%)</b>	2.45	3.63	10.92

Figure 2 shows the calculated Henry's law constants of R32, R134a and R1234yf in [C<sub>2</sub>mim][SCN] as a function of temperature, which are well-correlated with an Arrhenius type expression.

$$\ln k_H = \frac{A}{T} + B \quad (22)$$

These results are also provided as Supplementary Information in Table S5 and S6. According to Eq. (12), Henry's law constants increase with increasing temperature as solubility decreases. As can be seen, Figure 2 indicates that the effect of temperature on the solubility of R1234yf is larger than for the other two refrigerant gases. Accordingly, the solubility selectivity of R32 and R134a towards the HFO R1234yf is enhanced with temperature.

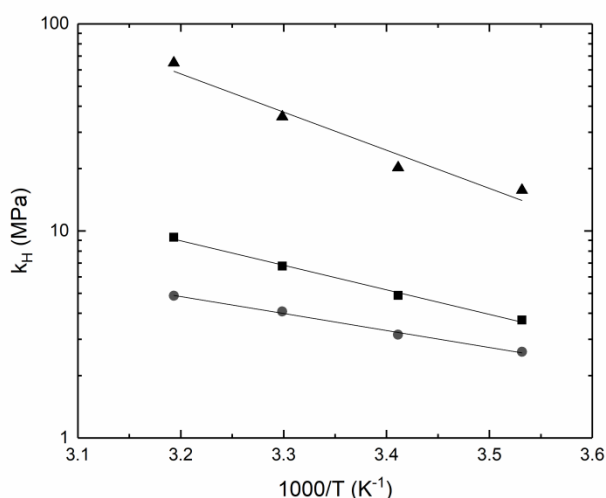


Figure 2. Henry's law constants for the absorption of R32 (●), R134a (■) and R1234yf (▲) in [C<sub>2</sub>mim][SCN] as a function of temperature. Solid lines represent the linear least-squares regressions.

### 3.2. Gas diffusivity

Regarding gas diffusivity, Figure 3 presents the value of diffusion coefficients at infinite dilution of the three refrigerants in [C<sub>2</sub>mim][SCN] between 283.15 and 313.15 K. In addition, data are provided in Table S7 as Supplementary Information. As can be seen, diffusivity in [C<sub>2</sub>mim][SCN] increases with temperature and the influence of temperature on the diffusion coefficients is well correlated with an Arrhenius type expression. Besides, selecting a low-viscosity IL such as [C<sub>2</sub>mim][SCN] enhances diffusivity of the gases as expected, so the diffusion coefficients of hydrofluorocarbons in [C<sub>2</sub>mim][SCN] obtained in this work are higher than those found in more viscous ILs [54,60], which is extremely important to reduce mass transfer resistance in this type of viscous fluids. Moreover, the activation energy of diffusion,  $E_D$ , derived from diffusivity data at infinite dilution is presented in Figure 4 as a function of the penetrant size. As expected, a strong influence is found between  $E_D$  and the molecular diameter of the refrigerants [61,62].

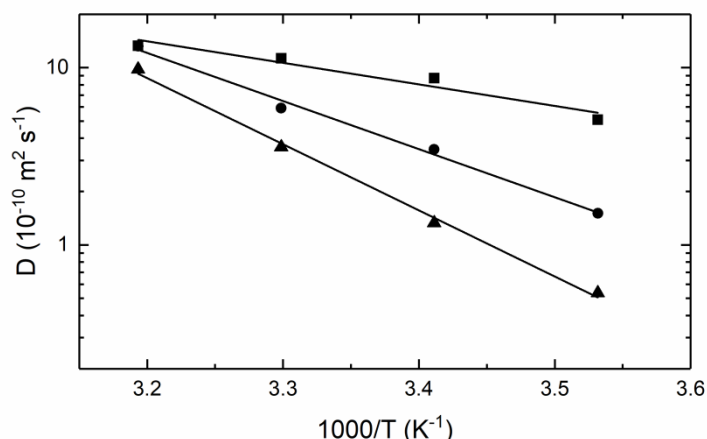


Figure 3. Influence of temperature on the diffusion coefficients at infinite dilution of refrigerant gases in  $[\text{C}_2\text{mim}][\text{SCN}]$ : R32 (■), R134a (●) and R1234yf (▲). Solid lines are the linear least-squares regressions.

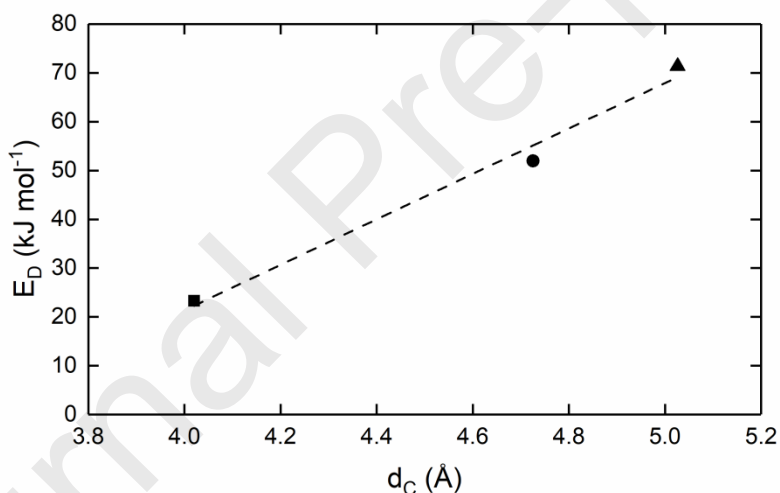


Figure 4. Relationship between the activation energy of diffusion and refrigerant Chung diameter [63] of R32 (■), R134a (●) and R1234yf (▲). Dashed line is a guide to the eye.

### 3.3. Thermodynamic separation assessment

The IL  $[\text{C}_2\text{mim}][\text{SCN}]$  presents significantly different absorption capacity for the three fluorinated compounds assessed (R32, R134a and R1234yf), which differs from other ILs in which higher and very similar absorption capacities for these gases are observed [18,26,28,46,49]. It is generally accepted that the high solubility of hydrofluorocarbons in ILs is associated with their H-bonding capability (H-F-H) [18,51,56,64]. In the present work, selecting the  $[\text{SCN}]$  anion moiety, without neither fluorine nor

hydrogen atoms, is aimed at avoiding hydrogen bonding between the refrigerant gas and the IL anion, thus limiting the penetrant-IL interactions in order to increase the typically low HFC/HFO solubility selectivity found in other ILs. In this regard, solubility differences observed among hydrofluorocarbon gases in [C<sub>2</sub>mim][SCN] could be related to their polar nature. However, the electric dipole moments of R32, R134a and R1234yf (1.649, 1.563 and 2.24 D, respectively [18,65]) do not correlate the observed solubility trend (R32 > R134a > R1234yf), a fact that is in good agreement with previous works [18]. Moreover, it has been reported that the effective dipolar moment of HFCs increases due to clusters formed by molecular associations between the gas molecules [18,66–68]. On the other hand, the electron-rich double bond of the R1234yf molecule may weaken the possibility of forming these clusters due to shielding effects of the C-H bonds that eventually reduce their potential to act as H-bond donors [69]. Thus, the formation of HFC molecular associations might contribute to the higher solubility of HFCs R32 and R134a with respect to the HFO R1234yf.

A deeper understanding of refrigerants solvation into ILs is gained by assessing the solvation enthalpy and entropy at infinite dilution, which are presented in Table S8 as Supplementary Information and in Figure 5. Solvation enthalpy reflects the energy of gas-IL interactions (hydrogen bonds, dipoles, Van der Waals forces), and solvation entropy is a measure of the degree of ordering of solvent molecules around the solute [55]. Figure 5 also shows a comparison between solvation energies of the three fluorinated gases in [C<sub>2</sub>mim][SCN] calculated in this work and in other ILs, which were derived from available absorption data in the literature [18,26,28,46,48,49]. As can be seen, there are larger differences between the solvation energies of R32, R134a and R1234yf in [C<sub>2</sub>mim][SCN] than in the other two ILs, which are consistent with the larger solubility differences observed between refrigerants in [C<sub>2</sub>mim][SCN]. Apart from the enthalpic effects discussed above, entropic effects can also play an important role regarding the solubility differences between hydrofluorocarbons in ILs [25]. In [C<sub>2</sub>mim][SCN], the biggest molecule R1234yf yields a less-ordered structure in solution, as evidenced by its more negative solvation entropy, what eventually leads to notably lower gas solubility [55]. Therefore, the comparison shown in Figure 5 also confirms the initial hypothesis that decreasing cation

alkyl chain length and anion size and avoiding fluorine substitution allows [C<sub>2</sub>mim][SCN] to improve the selective separation of HFCs from HFOs with respect to other ILs. In summary, the reduction in size and limiting fluorine substitution contribute to reducing the IL free volume, which hampers the accommodation of larger molecules such as the HFO R1234yf [24,70,71].

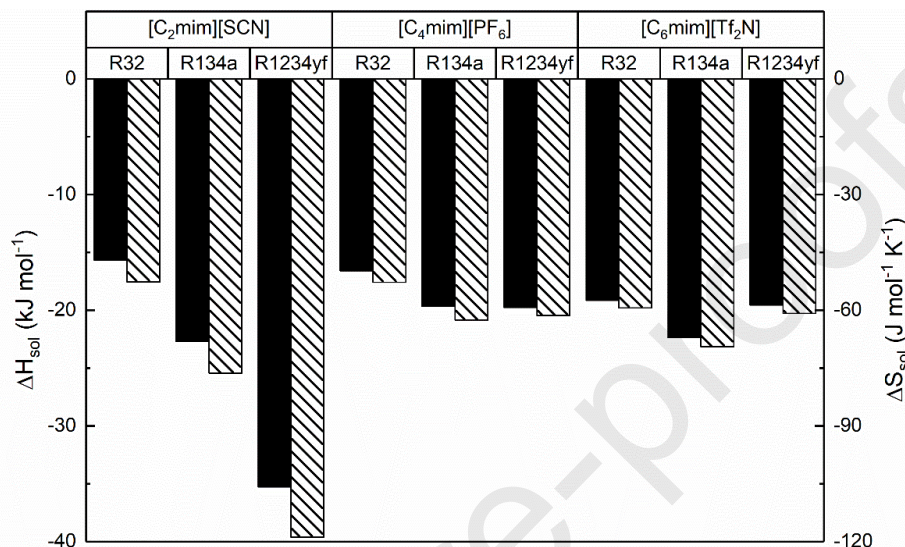


Figure 5. Comparison of solvation enthalpies (solid column) and entropies (striped column) of refrigerant gases in [C<sub>2</sub>mim][SCN] and other ILs [18,26,28,46,48,49].

Activity coefficients at infinite dilution and Gibbs free energy of mixing can be used to rationalize the solubility differences between these refrigerants. A certain compound is more soluble than ideal if  $\gamma_1^\infty < 1$ , and less soluble than ideal if  $\gamma_1^\infty > 1$ . Table 4 presents the results of  $\gamma_1^\infty$  at several temperatures, showing that the three gases are less soluble than ideal. Particularly, R1234yf is much less soluble than ideal, which is in accordance with the observed behavior. Likewise, the Gibbs free energy of mixing calculated with NRTL is presented in Figure S2 as Supplementary Information. The more negative the  $\Delta g^{mix}$ , the higher the sorption capacity, so the trends observed in Figure S2 are also consistent with experimental observations.

Table 4. Activity coefficients at infinite dilution of R32, R134a and R1234yf in [C<sub>2</sub>mim][SCN].

$T$ (K)	$\gamma_{R32}^{\infty}$	$\gamma_{R134a}^{\infty}$	$\gamma_{R1234yf}^{\infty}$
283.15	2.76	10.21	40.06
293.15	2.78	10.34	40.88
303.15	2.79	10.46	54.49
313.15	2.80	10.56	83.70

The observed solubility differences are promising for the design of absorption or extractive distillation processes aimed towards the selective separation and recovery of refrigerant fluorinated gases. Mixtures of R32 or R134a, both HFC refrigerant gases, with R1234yf, an HFO, are gaining importance as replacement for high GWP HFC mixtures affected by legislation. The recovery of these refrigerants employing advanced regeneration technologies will be key for companies in their adaptation to the new regulations. For a preliminary assessment of IL candidates, the ideal separation factors are a useful measure to determine theoretical separation performances of absorption systems [57]. Table 5 presents both the ideal selectivity at infinite dilution and the noncompetitive selectivity calculated at 0.5 MPa in the temperature range 283.15-313.15 K. R32/R1234yf and R134a/R1234yf selectivity are in the range 5-14 and 4-9, respectively, and increase with temperature. Therefore, further stages of process design will have to focus on analyzing the optimal separation conditions to reach a trade-off between the amount of solvent and the number of equilibrium stages required for a certain degree of separation.

Table 5. Ideal selectivity ( $S_{1/2}$ ) and noncompetitive absorption selectivity at 0.5 MPa ( $S_{1/2}^p$ ) in [C<sub>2</sub>mim][SCN].

$T$ (K)	283.15	293.15	303.15	313.15
$S_{R32/R1234yf}$	6.0	6.4	8.7	13.3
$S_{R32/R1234yf}^p$	5.1	5.5	7.5	14.2
$S_{R134a/R1234yf}$	4.2	4.0	5.3	7.0
$S_{R134a/R1234yf}^p$	4.5	4.0	4.9	8.6

Finally, the selectivity achieved with  $[\text{C}_2\text{mim}][\text{SCN}]$  is compared to that of other ILs in Figure 6 [18,19,26–28,46,48,49]. The comparison shows that the solubility selectivity of  $[\text{C}_2\text{mim}][\text{SCN}]$  for R32/R1234yf separation is at least twofold higher than in any other system. On the other hand, for the case of R134a/R1234yf separation, selectivity differences among ILs are smaller. Only  $[\text{C}_6\text{mim}][\text{BF}_4]$  at infinite dilution and  $[\text{C}_4\text{mim}][\text{PF}_6]$  at 0.5 MPa exhibit comparable selectivity to  $[\text{C}_2\text{mim}][\text{SCN}]$ , yet their viscosity is one order of magnitude higher (Table 2).

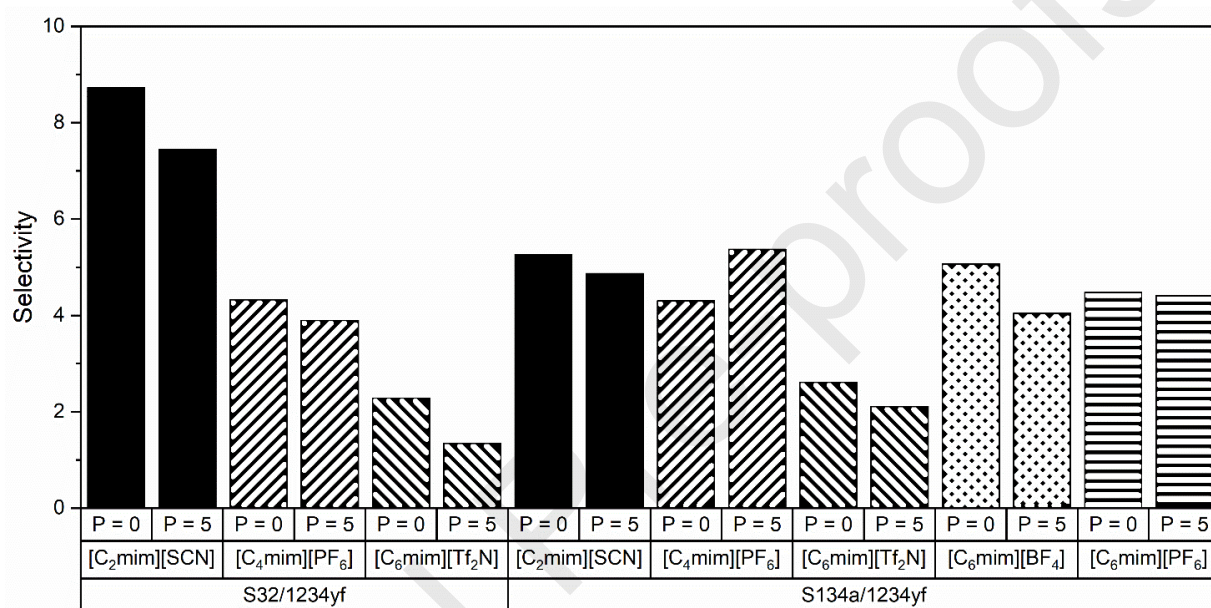


Figure 6. Comparison of R32/R1234yf and R134a/1234yf ideal selectivity at infinite dilution ( $P = 0$ ) and non-competitive selectivity at 0.5 MPa ( $P = 5$ ) in  $[\text{C}_2\text{mim}][\text{SCN}]$  (data from this work) and in other ILs ([18,19,26–28,46,48,49]).

#### 4. Conclusions

This work is directed towards the development of innovative technologies for the separation and recycling of hydrofluorocarbon refrigerant gases. Specifically, we have studied the absorption separation using ILs of the HFCs R32 and R134a, and the HFO R1234yf, which are among the main components of most of the new commercial refrigerants blends. The results obtained reveal that  $[\text{C}_2\text{mim}][\text{SCN}]$ , with a small and non-fluorinated anion, provides higher HFC/HFO sorption selectivity

than ILs with bigger molar volume and fluorinated anions. This fact can be ascribed to unfavorable entropic solvation effects that hinder the solvation of large molecules such as the HFO R1234yf in [C<sub>2</sub>mim][SCN]. In particular, for the gas pair R32/R1234yf, the solubility selectivity found in [C<sub>2</sub>mim][SCN] is 2-6 times higher (at 0.5 MPa) than that previously reported in any other IL, and up to twofold higher for the pair R134a/R1234yf. In addition, the phase behavior of the refrigerant-IL binary systems has been accurately modeled using the NRTL activity-coefficient method. Moreover, the diffusion coefficients of R32, R134a and R1234yf in [C<sub>2</sub>mim][SCN], in the range 10<sup>-9</sup>-10<sup>-10</sup> m<sup>2</sup> s<sup>-1</sup>, are also higher than those found in more viscous ILs, which is extremely important to overcome mass transfer limitations in kinetically controlled separation processes using ILs.

### Acknowledgements

This research is supported by Project KET4F-Gas – SOE2/P1/P0823, which is co-financed by the European Regional Development Fund within the framework of Interreg Sudoe Programme. S. A-D. and F.P. acknowledge the FPU grant (18/03939) and the post-doctoral fellowship (FJCI-2017-32884 Juan de la Cierva Formación), respectively, awarded by the Spanish Ministry of Science, Innovation and Universities.

### References

- [1] F. Graziosi, J. Arduini, F. Furlani, U. Giostra, P. Cristofanelli, X. Fang, O. Hermanssen, C. Lunder, G. Maenhout, S. O'Doherty, S. Reimann, N. Schmidbauer, M.K. Vollmer, D. Young, M. Maione, European emissions of the powerful greenhouse gases hydrofluorocarbons inferred from atmospheric measurements and their comparison with annual national reports to UNFCCC, *Atmos. Environ.* 158 (2017) 85–97. <https://doi.org/10.1016/j.atmosenv.2017.03.029>.
- [2] A. Mota-Babiloni, P. Makhnatch, R. Khodabandeh, Recent investigations in HFCs substitution with lower GWP synthetic alternatives: Focus on energetic performance and environmental impact, *Int. J. Refrig.* 82 (2017) 288–301. <https://doi.org/10.1016/j.ijrefrig.2017.06.026>.
- [3] A. Mota-Babiloni, J. Navarro-Esbrí, Á. Barragán-Cervera, F. Molés, B. Peris, Analysis based on EU Regulation No 517/2014 of new HFC/HFO mixtures as alternatives of high GWP refrigerants in refrigeration and HVAC systems, *Int. J. Refrig.* 52 (2015) 21–31. <https://doi.org/10.1016/j.ijrefrig.2014.12.021>.
- [4] N. Abas, A.R. Kalair, N. Khan, A. Haider, Z. Saleem, M.S. Saleem, Natural and synthetic refrigerants, global warming: A review, *Renew. Sustain. Energy Rev.* 90 (2018) 557–569.

- <https://doi.org/10.1016/j.rser.2018.03.099>.
- [5] European Parliament and Council, Regulation EU 517/2014, (2014) 195–230.
- [6] United Nations Environment Programme, Ratification of the Kigali Amendment, Ozone Secr. (2017).
- [7] United Nations, Amendment to the Montreal protocol on substances that deplete the ozone layer, (2016).
- [8] I.H. Bell, J. Wronski, S. Quoilin, V. Lemort, Pure and Pseudo-pure Fluid Thermophysical Property Evaluation and the Open-Source Thermophysical Property Library CoolProp, *Ind. Eng. Chem. Res.* 53 (2014) 2498–2508. <https://doi.org/10.1021/ie4033999>.
- [9] F. Pardo, G. Zarca, A. Urriaga, Separation of Refrigerant Gas Mixtures Containing R32, R134a, and R1234yf through Poly(ether- block -amide) Membranes, *ACS Sustain. Chem. Eng.* 8 (2020) 2548-2556. <https://doi.org/10.1021/acssuschemeng.9b07195>.
- [10] X. Hu, X. Meng, J. Wu, Isothermal vapor liquid equilibrium measurements for difluoromethane (R32) + trans-1,3,3,3-tetrafluoropropene (R1234ze(E)), *Fluid Phase Equilib.* 431 (2017) 58–65. <https://doi.org/10.1016/j.fluid.2016.10.011>.
- [11] X. Dong, H. Guo, M. Gong, Z. Yang, J. Wu, Measurements of isothermal (vapour + liquid) equilibria data for {1,1,2,2-Tetrafluoroethane (R134) + trans-1,3,3,3-tetrafluoropropene (R1234ze(E))} at T = (258.150 to 288.150) K, *J. Chem. Thermodyn.* 60 (2013) 25–28. <https://doi.org/10.1016/j.jct.2012.12.026>.
- [12] T. Kamiaka, C. Dang, E. Hihara, Vapor-liquid equilibrium measurements for binary mixtures of R1234yf with R32, R125, and R134a, *Int. J. Refrig.* 36 (2013) 965–971. <https://doi.org/10.1016/j.ijrefrig.2012.08.016>.
- [13] L. Kou, Z. Yang, X. Tang, W. Zhang, J. Lu, Experimental measurements and correlation of isothermal vapor-liquid equilibria for HFC-32 + HFO-1234ze (E) and HFC-134a + HFO-1234ze (E) binary systems, *J. Chem. Thermodyn.* 139 (2019) 105798. <https://doi.org/10.1016/j.jct.2019.04.020>.
- [14] M.B. Shiflett, A. Yokozeki, Separation of difluoromethane and pentafluoroethane by extractive distillation using ionic liquid, *Chem. Today.* 24 (2006) 28–30.
- [15] M.B. Shiflett, A.D. Shiflett, A. Yokozeki, Separation of tetrafluoroethylene and carbon dioxide using ionic liquids, *Sep. Purif. Technol.* 79 (2011) 357–364. <https://doi.org/10.1016/j.seppur.2011.03.023>.
- [16] G. Zarca, I. Ortiz, A. Urriaga, Recovery of carbon monoxide from flue gases by reactive absorption in ionic liquid imidazolium chlorocuprate(I): Mass transfer coefficients, *Chinese J. Chem. Eng.* 23 (2015) 769–774. <https://doi.org/10.1016/j.cjche.2014.06.040>.
- [17] G. Zarca, I. Ortiz, A. Urriaga, Kinetics of the carbon monoxide reactive uptake by an imidazolium chlorocuprate(I) ionic liquid, *Chem. Eng. J.* 252 (2014) 298–304. <https://doi.org/10.1016/j.cej.2014.05.011>.
- [18] M.B. Shiflett, A. Yokozeki, Solubility and Diffusivity of Hydrofluorocarbons in Room-Temperature Ionic Liquids, *AIChE J.* 52 (2006) 1205–1219. <https://doi.org/10.1002/aic.10685>.
- [19] Y. Sun, Y. Zhang, X. Wang, J.M. Prausnitz, L. Jin, Gaseous absorption of 2,3,3,3-tetrafluoroprop-1-ene in three imidazolium-based ionic liquids, *Fluid Phase Equilib.* 450 (2017) 65–74. <https://doi.org/10.1016/j.fluid.2017.07.013>.

- [20] M.B. Shiflett, A. Yokozeki, Absorption cycle utilizing ionic liquid as working fluid, US 8715521 B2, 2014.
- [21] C.J. Noelke, M.B. Shiflett, Capture of fluorinated vinyl monomers using ionic liquids, US 8,779,220 B2, 2014.
- [22] M.B. Shiflett, Capture of trifluoromethane using ionic liquids, US Patent Application 2015/0082981 A1, 2015.
- [23] D.L. Minnick, M.B. Shiflett, Solubility and Diffusivity of Chlorodifluoromethane in Imidazolium Ionic Liquids: [emim][Tf2N], [bmim][BF4], [bmim][PF6], and [emim][TFES], *Ind. Eng. Chem. Res.* 58 (2019) 11072–11081. <https://doi.org/10.1021/acs.iecr.9b02419>.
- [24] J.E. Sosa, R.P.P.L. Ribeiro, P.J. Castro, J.P.B. Mota, J.M.M. Araújo, A.B. Pereira, Absorption of Fluorinated Greenhouse Gases Using Fluorinated Ionic Liquids, *Ind. Eng. Chem. Res.* 58 (2019) 20769–20778. <https://doi.org/10.1021/acs.iecr.9b04648>.
- [25] L.F. Lepre, D. Andre, S. Denis-Quanquin, A. Gautier, A.A.H. Pádua, M.F. Costa Gomes, Ionic liquids can enable the recycling of fluorinated greenhouse gases, *ACS Sustain. Chem. Eng.* 7 (2019) 16900–16906. <https://doi.org/10.1021/acssuschemeng.9b04214>.
- [26] Y. Zhang, J. Yin, X. Wang, Vapor-liquid equilibrium of 2,3,3,3-tetrafluoroprop-1-ene with 1-butyl-3-methylimidazolium hexafluorophosphate, 1-hexyl-3-methyl imidazolium hexafluorophosphate, and 1-octyl-3-methylimidazolium hexafluorophosphate, *J. Mol. Liq.* 260 (2018) 203–208. <https://doi.org/10.1016/j.molliq.2018.03.112>.
- [27] X. Liu, Z. Ye, L. Bai, M. He, Performance comparison of two absorption-compression hybrid refrigeration systems using R1234yf/ionic liquid as working pair, *Energy Convers. Manag.* 181 (2019) 319–330. <https://doi.org/10.1016/j.enconman.2018.12.030>.
- [28] X. Liu, M. He, N. Lv, X. Qi, C. Su, Vapor–Liquid Equilibrium of Three Hydrofluorocarbons with [HMIM][Tf2N], *J. Chem. Eng. Data.* 60 (2015) 1354–1361. <https://doi.org/10.1021/je501069b>.
- [29] M.B. Shiflett, A. Yokozeki, Vapor-Liquid-Liquid Equilibria of Hydrofluorocarbons + 1-Butyl-3-methylimidazolium Hexafluorophosphate, *J. Chem. Eng. Data.* 51 (2006) 1931–1939. <https://doi.org/10.1021/je060275f>.
- [30] M.B. Shiflett, A. Yokozeki, Gaseous Absorption of Fluoromethane, Fluoroethane, and 1,1,2,2-Tetrafluoroethane in 1-Butyl-3-Methylimidazolium Hexafluorophosphate, *Ind. Eng. Chem. Res.* 45 (2006) 6375–6382. <https://doi.org/10.1021/ie060192s>.
- [31] M.B. Shiflett, M.A. Harmer, C.P. Junk, A. Yokozeki, Solubility and diffusivity of 1,1,1,2-tetrafluoroethane in room-temperature ionic liquids, *Fluid Phase Equilib.* 242 (2006) 220–232. <https://doi.org/10.1016/j.fluid.2006.01.026>.
- [32] M.B. Shiflett, A. Yokozeki, Solubility Differences of Halocarbon Isomers in Ionic Liquid [emim][Tf2N], *J. Chem. Eng. Data.* 52 (2007) 2007–2015. <https://doi.org/10.1021/je700295e>.
- [33] M.B. Shiflett, A. Yokozeki, Utilizing ionic liquids for hydrofluorocarbon separation, US 9,628,644 B2, 2014.
- [34] J. Palomar, M. Larriba, J. Lemus, D. Moreno, R. Santiago, C. Moya, J. de Riva, G. Pedrosa, Demonstrating the key role of kinetics over thermodynamics in the selection of ionic liquids for CO<sub>2</sub> physical absorption, *Sep. Purif. Technol.* 213 (2019) 578–586. <https://doi.org/10.1016/j.seppur.2018.12.059>.
- [35] G. Zarca, I. Ortiz, A. Urriaga, Novel solvents based on thiocyanate ionic liquids doped with

- copper(I) with enhanced equilibrium selectivity for carbon monoxide separation from light gases, *Sep. Purif. Technol.* 196 (2018) 47–56. <https://doi.org/10.1016/j.seppur.2017.06.069>.
- [36] M.G. Freire, A.R.R. Teles, M.A.A. Rocha, B. Schröder, C.M.S.S. Neves, P.J. Carvalho, D. V. Evtuguin, L.M.N.B.F. Santos, J.A.P. Coutinho, Thermophysical Characterization of Ionic Liquids Able To Dissolve Biomass, *J. Chem. Eng. Data.* 56 (2011) 4813–4822. <https://doi.org/10.1021/je200790q>
- [37] D. Song, J. Chen, Density and viscosity data for mixtures of ionic liquids with a common anion, *J. Chem. Eng. Data.* 59 (2014) 257–262. <https://doi.org/10.1021/je400332j>.
- [38] J.A. Widegren, J.W. Magee, Density, viscosity, speed of sound, and electrolytic conductivity for the ionic liquid 1-hexyl-3-methylimidazolium bis(trifluoromethylsulfonyl)imide and its mixtures with water, *J. Chem. Eng. Data.* 52 (2007) 2331–2338. <https://doi.org/10.1021/je700329a>.
- [39] K.R. Harris, M. Kanakubo, L.A. Woolf, Temperature and pressure dependence of the viscosity of the ionic liquid 1-butyl-3-methylimidazolium tetrafluoroborate: Viscosity and density relationships in ionic liquids, *J. Chem. Eng. Data.* 52 (2007) 2425–2430. <https://doi.org/10.1021/je700370z>.
- [40] W. Fan, Q. Zhou, J. Sun, S. Zhang, Density, excess molar volume, and viscosity for the methyl methacrylate + 1-butyl-3-methylimidazolium hexafluorophosphate ionic liquid binary system at atmospheric pressure, *J. Chem. Eng. Data.* 54 (2009) 2307–2311. <https://doi.org/10.1021/je900091b>.
- [41] C.M.S.S. Neves, K.A. Kurnia, J.A.P. Coutinho, I.M. Marrucho, J.N.C. Lopes, M.G. Freire, L.P.N. Rebelo, Systematic study of the thermophysical properties of imidazolium-based ionic liquids with cyano-functionalized anions, *J. Phys. Chem. B.* 117 (2013) 10271–10283. <https://doi.org/10.1021/jp405913b>.
- [42] B. Hasse, J. Lehmann, D. Assenbaum, P. Wasserscheid, A. Leipertz, A.P. Fröba, Viscosity, Interfacial Tension, Density, and Refractive Index of Ionic Liquids [EMIM][MeSO<sub>3</sub>], [EMIM][MeOHPO<sub>2</sub>], [EMIM][OcSO<sub>4</sub>], and [BBIM][NTf<sub>2</sub>] in Dependence on Temperature at Atmospheric Pressure, *J. Chem. Eng. Data.* 54 (2009) 2576–2583. <https://doi.org/10.1021/je900134z>
- [43] Y.A. Sanmamed, D. González-Salgado, J. Troncoso, L. Romani, A. Baylaucq, C. Boned, Experimental methodology for precise determination of density of RTILs as a function of temperature and pressure using vibrating tube densimeters, *J. Chem. Thermodyn.* 42 (2010) 553–563. <https://doi.org/10.1016/j.jct.2009.11.014>.
- [44] M.A.A. Rocha, F.M.S. Ribeiro, A.I.M.C.L. Ferreira, J.A.P. Coutinho, L.M.N.B.F. Santos, Thermophysical properties of [CN - 1C1im][PF 6] ionic liquids, *J. Mol. Liq.* 188 (2013) 196–202. <https://doi.org/10.1016/j.molliq.2013.09.031>.
- [45] A. Hofmann, M. Migeot, T. Hanemann, Investigation of Binary Mixtures Containing 1-Ethyl-3-methylimidazolium Bis(trifluoromethanesulfonyl)azanide and Ethylene Carbonate, *J. Chem. Eng. Data.* 61 (2016) 114–123. <https://doi.org/10.1021/acs.jced.5b00338>.
- [46] W. Ren, A.M. Scurto, Phase equilibria of imidazolium ionic liquids and the refrigerant gas, 1,1,1,2-tetrafluoroethane (R-134a), *Fluid Phase Equilib.* 286 (2009) 1–7. <https://doi.org/10.1016/j.fluid.2009.07.007>.
- [47] M.B. Shiflett, M.A. Harmer, C.P. Junk, A. Yokozeki, Solubility and Diffusivity of Difluoromethane in Room-Temperature Ionic Liquids, *J. Chem. Eng. Data.* 51 (2006) 483–495. <https://doi.org/10.1021/je050386z>.

- [48] A. Aghosseini, W. Ren, L.R. Weatherley, A.M. Scurto, Viscosity and self-diffusivity of ionic liquids with compressed hydrofluorocarbons: 1-Hexyl-3-methyl-imidazolium bis(trifluoromethylsulfonyl)amide and 1,1,1,2-tetrafluoroethane, *Fluid Phase Equilib.* 437 (2017) 34–42. <https://doi.org/10.1016/j.fluid.2016.11.022>.
- [49] X. Liu, L. Bai, S. Liu, M. He, Vapor–Liquid Equilibrium of R1234yf/[HMIM][Tf2N] and R1234ze (E)/[HMIM][Tf2N] Working Pairs for the Absorption Refrigeration Cycle, *J. Chem. Eng. Data.* 61 (2016) 3952–3957. <https://doi.org/10.1021/acs.jced.6b00731>.
- [50] J.D. Seader, E.J. Henley, D.K. Roper, *Separation process principles*, 3rd ed, John Wiley & Sons, Ltd, New Jersey, USA, 2010.
- [51] L. Dong, D. Zheng, G. Sun, X. Wu, Vapor-Liquid Equilibrium Measurements of Difluoromethane + [Emim]OTf, Difluoromethane + [Bmim]OTf, Difluoroethane + [Emim]OTf, and Difluoroethane + [Bmim]OTf Systems, *J. Chem. Eng. Data.* 56 (2011) 3663–3668.
- [52] J. Crank, *The Mathematics of Diffusion*, 2nd ed, Clarendon Press, Oxford, UK, 1975. [https://doi.org/10.1016/0306-4549\(77\)90072-X](https://doi.org/10.1016/0306-4549(77)90072-X).
- [53] D. Camper, C. Becker, C. Koval, R. Noble, Diffusion and solubility measurements in room temperature ionic liquids, *Ind. Eng. Chem. Res.* 45 (2006) 445–450. <https://doi.org/10.1021/ie0506668>.
- [54] M. He, S. Peng, X. Liu, P. Pan, Y. He, Diffusion coefficients and Henry’s constants of hydrofluorocarbons in [HMIM][Tf2N], [HMIM][TfO], and [HMIM][BF4], *J. Chem. Thermodyn.* 112 (2017) 43–51. <https://doi.org/10.1016/j.jct.2017.04.009>.
- [55] L. Moura, W. Darwich, C.C. Santini, M.F. Costa Gomes, Imidazolium-based ionic liquids with cyano groups for the selective absorption of ethane and ethylene, *Chem. Eng. J.* 280 (2015) 755–762. <https://doi.org/10.1016/j.cej.2015.06.034>.
- [56] D. Almantariotis, T. Gefflaut, A.A.H. Pádua, J.-Y. Coxam, M.F. Costa Gomes, Effect of fluorination and size of the alkyl side-chain on the solubility of carbon dioxide in 1-alkyl-3-methylimidazolium bis(trifluoromethylsulfonyl) amide ionic liquids, *J. Phys. Chem. B.* 114 (2010) 3608–3617. <https://doi.org/10.1021/jp912176n>.
- [57] J. Blath, M. Christ, N. Deubler, T. Hirth, T. Schiestel, Gas solubilities in room temperature ionic liquids - Correlation between RTIL-molar mass and Henry’s law constant, *Chem. Eng. J.* 172 (2011) 167–176. <https://doi.org/10.1016/j.cej.2011.05.084>.
- [58] P.J. Carvalho, K.A. Kurnia, J.A.P. Coutinho, Dispelling some myths about the CO<sub>2</sub> solubility in ionic liquids, *Phys. Chem. Chem. Phys.* 18 (2016) 14757–14771. <https://doi.org/10.1039/c6cp01896c>.
- [59] Y. Sun, Y. Zhang, G. Di, X. Wang, J.M. Prausnitz, L. Jin, Vapor-Liquid Equilibria for R1234ze(E) and Three Imidazolium-Based Ionic Liquids as Working Pairs in Absorption-Refrigeration Cycle, *J. Chem. Eng. Data.* 63 (2018) 3053–3060. <https://doi.org/10.1021/acs.jced.8b00314>.
- [60] X. Liu, P. Pan, M. He, Vapor-liquid equilibrium and diffusion coefficients of R32 + [HMIM][FEP], R152a + [HMIM][FEP] and R161 + [HMIM][FEP], *J. Mol. Liq.* 253 (2018) 28–35. <https://doi.org/10.1016/j.molliq.2018.01.032>.
- [61] R. Condemarin, P. Scovazzo, Gas permeabilities, solubilities, diffusivities, and diffusivity correlations for ammonium-based room temperature ionic liquids with comparison to imidazolium and phosphonium RTIL data, *Chem. Eng. J.* 147 (2009) 51–57. <https://doi.org/10.1016/j.cej.2008.11.015>.

- [62] Y. Yampolskii, I. Pinnau, B. Freeman, *Materials science of membranes for gas and vapor separation*, John Wiley & Sons, Ltd, West Sussex, 2006.
- [63] T.-H. Chung, M. Ajlan, L.L. Lee, K.E. Starling, Generalized Multiparameter Correlation for Nonpolar and Polar Fluid Transport Properties, *Ind. Eng. Chem. Res.* 27 (1988) 671–679. <https://doi.org/10.1021/ie00076a024>.
- [64] X. Liu, M.Q. Nguyen, S. Xue, C. Song, M. He, Vapor-Liquid Equilibria and Inter-Diffusion Coefficients for Working Pairs for Absorption Refrigeration Systems Composed of [HMIM][BF<sub>4</sub>] and Fluorinated Propanes, *Int. J. Refrig.* 104 (2019) 34–41. <https://doi.org/10.1016/j.ijrefrig.2019.04.023>.
- [65] C.C. Sampson, M. Kamson, M.G. Hopkins, P.L. Stanwix, E.F. May, Dielectric permittivity, polarizability and dipole moment of refrigerants R1234ze(E) and R1234yf determined using a microwave re-entrant cavity resonator, *J. Chem. Thermodyn.* 128 (2019) 148–158. <https://doi.org/10.1016/j.jct.2018.07.011>.
- [66] B.J. Costa Cabral, R.C. Guedes, R.S. Pai-Panandiker, C.A. Nieto de Castro, Hydrogen bonding and the dipole moment of hydrofluorocarbons by density functional theory, *Phys. Chem. Chem. Phys.* 3 (2001) 4200–4207. <https://doi.org/10.1039/b102879k>.
- [67] E. Kryachko, S. Scheiner, CH...F hydrogen bonds. Dimers of fluoromethanes, *J. Phys. Chem. A.* 108 (2004) 2527–2535. <https://doi.org/10.1021/jp0365108>.
- [68] M. Karamoddin, F. Varaminian, Solubility of R22, R23, R32, R134a, R152a, R125 and R744 refrigerants in water by using equations of state, *Int. J. Refrig.* 36 (2013) 1681–1688. <https://doi.org/10.1016/j.ijrefrig.2013.04.013>.
- [69] I. Skarmoutsos, P.A. Hunt, Structural and dynamic properties of the new alternative refrigerant 2,3,3,3-tetrafluoro-1-propene (HFO-1234yf) in the liquid state, *J. Phys. Chem. B.* 114 (2010) 17120–17127. <https://doi.org/10.1021/jp108647p>.
- [70] M.L. Ferreira, J.M.M. Araújo, A.B. Pereiro, L.F. Vega, Insights into the influence of the molecular structures of fluorinated ionic liquids on their thermophysical properties. A soft-SAFT based approach, *Phys. Chem. Chem. Phys.* 21 (2019) 6362–6380. <https://doi.org/10.1039/c8cp07522k>.
- [71] T. Endo, Y. Nishisaka, Y. Kin, Y. Kimura, Systematic estimation and interpretation of fractional free volume in 1-alkyl-3-methylimidazolium-based ionic liquids, *Fluid Phase Equilib.* 498 (2019) 144–150. <https://doi.org/10.1016/j.fluid.2019.06.027>.

**Highlights**

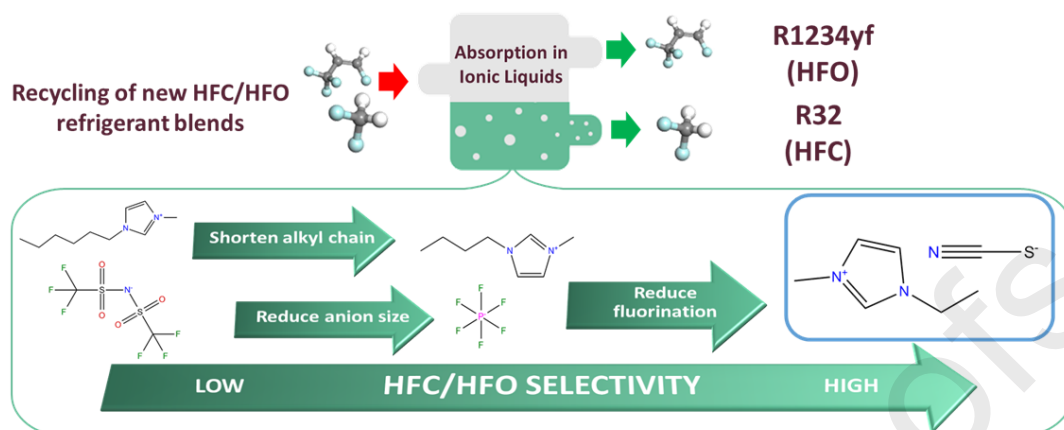
Ionic liquids can enable the recovery of HFCs and HFOs from refrigerant mixtures

Small size and low fluorinated ionic liquids enhance HFC/HFO solubility selectivity

High diffusion coefficients of hydrofluorocarbons in low-viscosity [C<sub>2</sub>mim][SCN]

Phase behavior accurately parametrized with NRTL activity model

Journal Pre-proofs



The authors declare that they have no conflict of interest.

Journal Pre-proofs

**AUTHORSHIP STATEMENT**

**Salvador Asensio-Delgado:** Investigation, Visualization, Writing - Original Draft; **Fernando Pardo:** Supervision, Writing - Review & Editing; **Gabriel Zarca:** Conceptualization, Writing - Review & Editing, Funding acquisition; **Ane Urtiaga:** Conceptualization, Writing - Review & Editing, Funding acquisition

Journal Pre-proofs